

Nanoscale Cu₂O Films: Radio-Frequency Magnetron Sputtering and Structural and Optical Studies

D. A. Kudryashov^{a*}, A. S. Gudovskikh^{a,b}, A. V. Babichev^{c,d,e}, A. V. Filimonov^c, A. M. Mozharov^a,
V. F. Agekyan^f, E. V. Borisov^f, A. Yu. Serov^f, and N. G. Filosofov^f

^a St. Petersburg National Research Academic University — Nanotechnology Research and Education Center,
Russian Academy of Sciences, St. Petersburg, 194021 Russia

^b St. Petersburg State Electrotechnical University LETI, St. Petersburg, 197376 Russia

^c Connector Optics LLC, St. Petersburg, 194292 Russia

^d St. Petersburg National Research University of Information Technologies, Mechanics, and Optics,
St. Petersburg, 197101 Russia

^e Ioffe Physical–Technical Institute, Russian Academy of Sciences, St. Petersburg, 194021 Russia

^f St. Petersburg State University, St. Petersburg, 199034 Russia

*e-mail: kudryashovda@apbau.ru

Submitted May 10, 2016; accepted for publication May 18, 2016

Abstract—Nanoscale copper (I) oxide layers are formed by magnetron-assisted sputtering onto glassy and silicon substrates in an oxygen-free environment at room temperature, and the structural and optical properties of the layers are studied. It is shown that copper oxide formed on a silicon substrate exhibits a lower degree of disorder than that formed on a glassy substrate, which is supported by the observation of a higher intensity and a smaller half-width of reflections in the diffraction pattern. The highest intensity of reflections in the diffraction pattern is observed for Cu₂O films grown on silicon at a magnetron power of 150 W. The absorption and transmittance spectra of these Cu₂O films are in agreement with the well-known spectra of bulk crystals. In the Raman spectra of the films, phonons inherent in the crystal lattice of cubic Cu₂O crystals are identified.

DOI: 10.1134/S1063782617010110

1. INTRODUCTION

In recent years, interest has grown in studies of metal-oxide semiconductors and heterojunctions on their basis for applications in light-emitting diodes, spintronic devices, and solar cells (SCs). In this group of semiconductors, copper (I) oxide is one of the most attractive materials from the standpoint of photovoltaics because of its nontoxicity and low price. Copper (I) oxide (Cu₂O) is a direct-gap, usually *p*-type semiconductor, with a band gap of about 2.2 eV; the absorption coefficient of copper (I) oxide reaches 10⁵ at about 2.6 eV [1]. The theoretically calculated Shockley–Queisser limit efficiency of SCs based on copper (I) oxide is about 20% [2]. However, at present, it is impossible to attain a high efficiency because of the problem of the production of Cu₂O films with a low content of defects. By the beginning of 2016, the experimentally attained efficiency of SCs based on the ZnO/Cu₂O oxide heterostructure is 6% [3], whereas the efficiency attained in 2009 was only 1%. The main reasons for a low efficiency are the small values of the short-circuit current and fill factor [4]. In ZnO/Cu₂O heterostructures, the main photocurrent losses occur

in the copper-oxide bulk and at the heterointerface because of a high concentration of recombination centers. The small value of the fill factor is a consequence of a low charge-carrier concentration in the light-absorbing layer. In [5], a two-dimensional computer model of a SC based on a Cu₂O/ZnO oxide heterostructure is presented; as the input data in this model, the experimentally determined characteristics of oxide semiconductors were used. This made it possible to estimate the maximal attainable efficiency of a SC based on the ZnO/Cu₂O heterostructure at 12% upon illumination by an AM 1.5 source with the power density 10 mW cm⁻²; in this case, the short-circuit current was 10 mA cm⁻².

To form copper (I) oxide, a number of methods are used. Among these, the most common method is the high-temperature oxidation of copper in an oxygen environment. Cu₂O films grown by this method are distinguished by their high-quality crystal structure [6] and a hole mobility that can reach 110 cm² V⁻¹ s⁻¹. However, the high-temperature of formation (above 1000°C) and difficult-to-control additional oxidation of the layers to CuO limit the field of application of

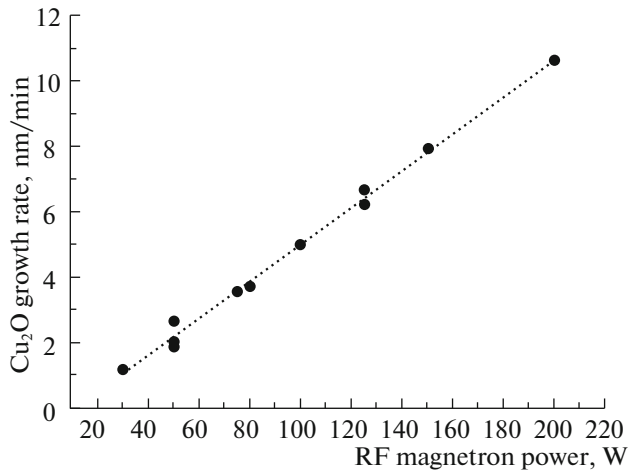


Fig. 1. Dependence of the Cu_2O deposition rate on the magnetron power. Circles and dotted line refer to the experimental data and their approximation, respectively.

such an approach. It is known that one of the main factors that assist in reducing the cost of SC production is the lowering of the temperature of the technological process. In addition, high temperatures (above 400°C) are often responsible for degradation of the individual components of SCs. This is specifically true for silicon which can be potentially used for the production of a two-junction SC based on the $\text{Cu}_2\text{O}/\text{Si}$ structure. It should be noted that the Cu_2O bulk crystals are cubic (the symmetry group O_h^4), whereas the films can be orthorhombic [7].

The magnetron-assisted sputtering technique does not require high temperatures for Cu_2O formation and allows the use of different materials as substrates, including so-called flexible substrates. During magnetron-assisted sputtering, it is possible to precisely control the parameters of the growing film by varying the magnetron power and the composition of the gas mixture in the chamber.

The purpose of this study is to form nanoscale copper (I) oxide (cuprous oxide) films on glassy and silicon substrates by magnetron-assisted sputtering and to explore the structural and optical properties of the films.

2. EXPERIMENTAL

To form copper (I) oxide nanolayers, we used a BOC EDWARDS auto 500RF setup for radio-frequency (RF) magnetron sputtering. The Cu_2O nanolayers were deposited onto single-crystal Si(100) and glassy substrates. During layer growth, the substrate temperature was not elevated above 40°C . As the working gas, we used high-purity (99.9995%) argon; the argon pressure in the working chamber was 0.18 Pa. The target was a disk made from sintered

high-purity (99.9%) Cu_2O (produced at Testbourne Ltd.); the disk was 5 mm in thickness and 3 in. in diameter. The rotational velocity of the holder with samples was 60 rpm. The thicknesses of the growing layers were determined with an AMBIOS XP-1 profilometer. The reflectance and transmittance spectra were recorded using Solar Laser Systems M266 and MDR-206-2 spectrometers. The film surfaces were analyzed with a Zeiss SUPRA 25 scanning electron microscope (SEM). The X-ray diffraction (XRD) spectra were obtained using a PANalytical X'PertPro setup in the $\theta-2\theta$ mode of scanning. Raman scattering of the Cu_2O nanolayers was studied with a CENTERRA (Bruker) spectrometer in the backscattering layout of the experiment; for comparison, under the same conditions, we recorded the Raman spectra of Cu_2O bulk crystals.

3. RESULTS AND DISCUSSION

From Fig. 1, it can be seen that the copper (I) oxide deposition rate linearly depends on the magnetron power. The copper (I) oxide films formed on silicon substrates exhibit a sharp interface and a comparatively smooth surface (Fig. 2). It is established that, at all sputtering powers used in the study, a barely noticeable column structure can be seen in the transverse cleavage of the copper (I) oxide. Such morphology is often observed in the case of the low-temperature magnetron-assisted deposition of oxides [2, 8], which is a consequence of the low mobility of deposited particles on the substrate surface.

3.1. XRD

The XRD data for the copper (I) oxide layers are shown in Fig. 3. It is evident that the highest intensity of reflections for a Cu_2O layer formed on a glassy substrate is observed at a magnetron power of 125 W. If a silicon substrate is used, the highest intensity of reflections is observed for the sample formed at a power of 150 W. It should be noted that, for a stoichiometric and strain-free copper (I) oxide crystal, the maxima of the rocking curve are observed at the angles 36.45° and 42.33° for the (111) and (200) planes, respectively [9]. In the case under study, these maxima are shifted to larger angles, which can be indicative of deviations from the stoichiometric composition. In fact, Cu_2O formation was conducted in an argon atmosphere without the addition of oxygen, and during bombardment of the Cu_2O target, a portion of oxygen atoms did not reach the substrate because of their high chemical activity. In such conditions, a copper (I) oxide layer depleted of oxygen is formed.

From Fig. 3, it is evident that the half-width of reflections from Cu_2O layers deposited on glassy substrates is considerably larger than that in the case of a

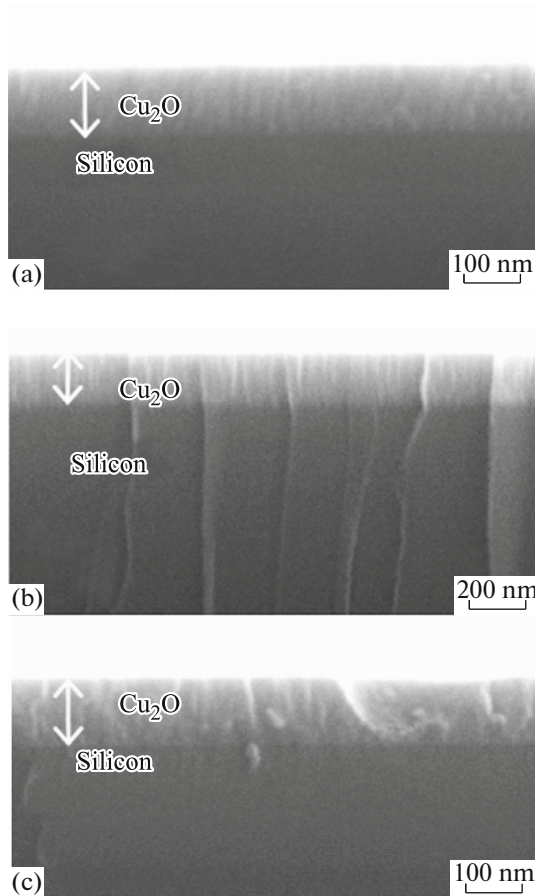


Fig. 2. SEM images of Cu_2O films deposited onto Si substrates at the magnetron powers (a) 80, (b) 125, and (c) 200 W.

silicon substrate. This is indicative of the higher degree of disorder of the copper oxide layer formed on the glass.

3.2. Optical Transmittance

In the spectra of Cu_2O bulk crystals, four interband transitions that involve two valence bands and two conduction bands are observed. Two optical transitions at energies of about 2.2 and 2.3 eV are dipole-forbidden; strong dipole absorption starts from about 2.6 eV, at which the absorption coefficient reaches 10^5 cm^{-1} . Figure 4 shows the transmittance spectra of Cu_2O layers fabricated in this study and the reflectance spectrum of a bulk crystal, in which an excitonic structure adjacent to the edges of two dipole-allowed band-to-band transitions is observed. It can be seen that the transmittance spectrum of the cuprous oxide layer grown at a magnetron power of 150 W satisfactorily correlates with the spectrum of the bulk crystal, in contrast to the spectra of layers grown at lower or higher powers of magnetron sputtering.

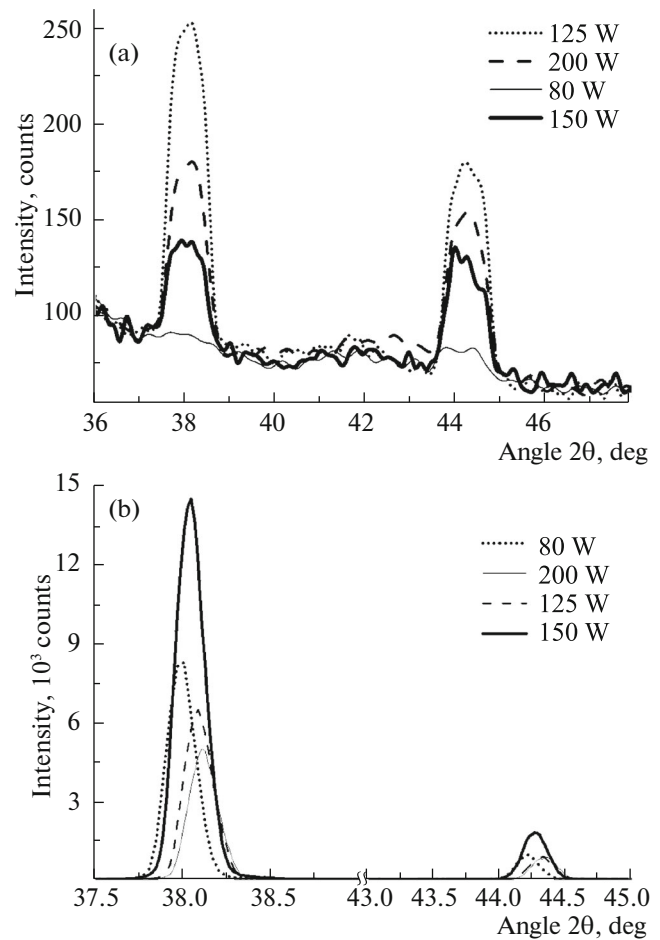


Fig. 3. XRD rocking curve for 150-nm-thick Cu_2O samples deposited on (a) glassy and (b) silicon substrates. The magnetron powers are indicated at the top right of the curves.

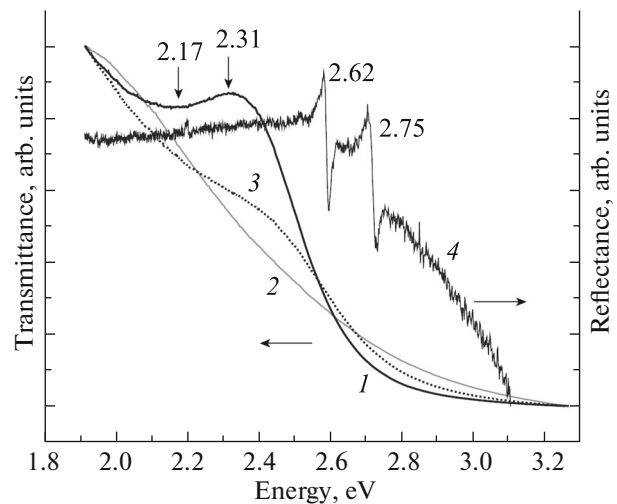


Fig. 4. Transmittance spectra of Cu_2O films grown on glassy substrates at the magnetron sputtering powers (1) 125, (2) 250, and (3) 50 W and (4) the reflectance spectrum of the Cu_2O bulk crystal. The indicated energies of interband transitions in Cu_2O are expressed in eV. $T = 80 \text{ K}$.

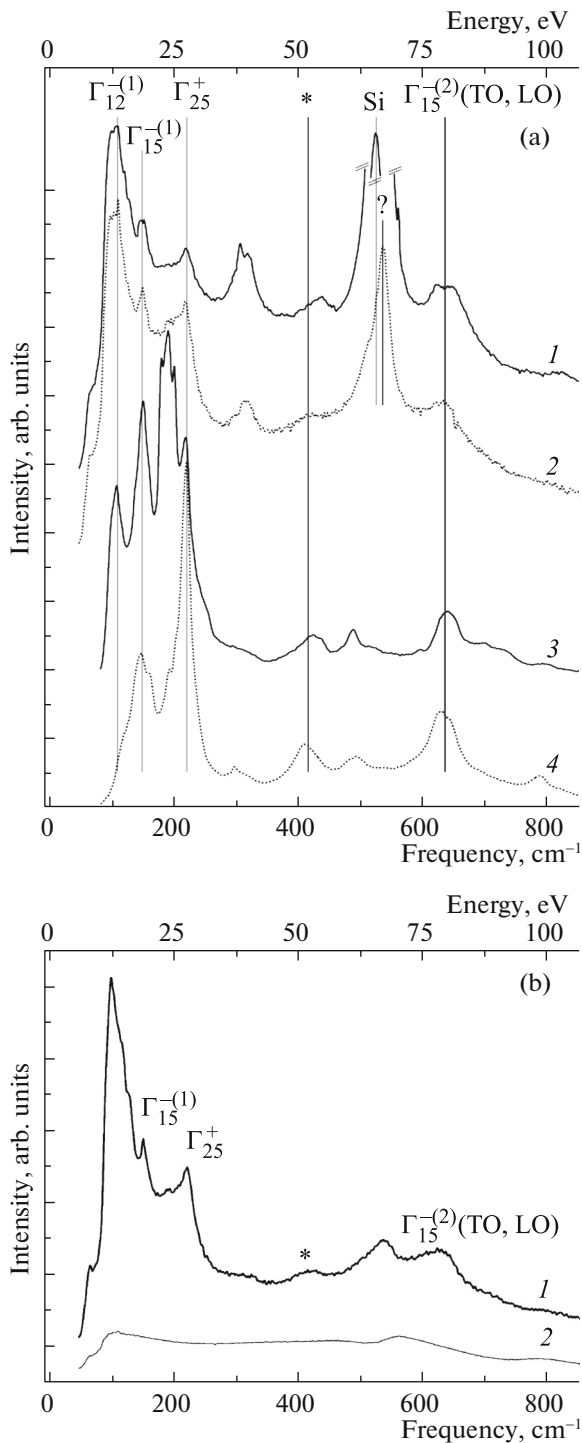


Fig. 5. Raman scattering spectra at room temperature. (a) (1, 2) the Cu₂O films grown (1) on silicon at the magnetron power 150 W and (2) on glass at the magnetron power 125 W upon excitation with a laser emitting at the photon energy 2.33 eV (Si denotes the Raman component of silicon); (3, 4) the Cu₂O bulk crystal excited with lasers emitting at the photon energies (3) 1.58 and (4) 2.54 eV, correspondingly, below and above the fundamental absorption edge. (b) (1) the Cu₂O film grown on glass at the magnetron power 160 W and (2) the glassy substrate upon excitation with a laser emitting at the photon energy 2.33 eV. The symmetry of optical phonons is indicated near the corresponding Raman components.

3.3. Raman Scattering

Raman scattering in cuprous oxide crystals was explored in a number of studies [10–14]. As a rule, Raman scattering was excited with lasers emitting at photon energies higher than the energy of the edge of the first interband transition; in such conditions, along with standard Raman modes, other modes, specifically, dipole-active modes are evident in the scattering spectra. It is worth noting that the cubic Cu₂O crystal lattice exhibits an inversion center and, in the case of nonresonant scattering, only the Raman mode is bound to be evident in the spectrum.

The Raman spectra of the Cu₂O single crystal and the layers grown on glassy and silicon substrates by magnetron-assisted sputtering are shown in Fig. 5. In these spectra, we can identify the Stokes components corresponding to the Γ_{25}^+ Raman phonon (220 cm⁻¹) and to the $\Gamma_{15}^{-(1)}$ (150 cm⁻¹) and $\Gamma_{15}^{-(2)}$ transverse optical (TO, 630 cm⁻¹) and longitudinal optical (LO, 660 cm⁻¹) dipole phonons. The $\Gamma_{15}^{-(2)}$ -symmetry vibration is the principal ion mode of the crystal. In the scattering spectra of Cu₂O films, the Γ_{25}^- (515–545 cm⁻¹), Γ_2^- (308 cm⁻¹), and Γ_3^- (110 cm⁻¹) phonons are evident. Thus, the Raman spectra of the Cu₂O layers produced by magnetron-assisted sputtering are indicative of their well-pronounced cubic crystal structure.

4. CONCLUSIONS

By magnetron-assisted sputtering, copper (I) oxide nanolayers are formed on glassy and silicon substrates in an oxygen-free environment at room temperature. The structural and optical properties of the nanolayers are studied. It is shown that the formation of copper oxide on a silicon substrate occurs with a lower degree of disorder compared to formation on a glassy substrate. This is supported by the observation of a higher intensity and a smaller half-width of reflections in the XRD pattern. The highest intensity of reflections in the XRD pattern is observed for the Cu₂O films grown on silicon at the magnetron power 150 W. The transmittance and Raman scattering spectra of these films are consistent with the spectra of cubic Cu₂O bulk crystals.

ACKNOWLEDGMENTS

The study was supported in part by the Russian Foundation for Basic Research, project no. 15-08-06645A, and the Presidium of the Russian Academy of Sciences, program no. 1, project no. 1.3.3.3.

REFERENCES

1. H. Wayne Richardson, *Copper Compounds in Ullmann's Encyclopedia of Industrial Chemistry* (Wiley-VCH, Weinheim, 2002).
2. Yun Seog Lee, M. T. Winkler, S. Cheng Siah, R. Brandt, and T. Buonassisi, *Appl. Phys. Lett.* **98**, 192115 (2011).
3. T. Minami, T. Miyata, and Y. Nishi, *Sol. Energy Mater. Solar Cells* **147**, 85 (2016).
4. T. Minami, T. Miyata, and Y. Nishi, *Thin Solid Films* **559**, 105 (2014).
5. D. A. Kudryashov and A. S. Gudovskikh, in *Proceedings of the E-MRS Spring Meeting 2015*, Lille, France, May 11–15, 2015.
6. T. Minami, Y. Nishi, T. Miyata, and Jun-ichi Nomoto, *Appl. Phys. Express* **4**, 062301 (2011).
7. Y. Sun, K. Rivkin, J. Chen, J. D. Ketterson, P. Markworth, and R. P. Chang, *Phys. Rev. B* **66**, 245315 (2002).
8. R. Subba Reddy, K. Radhama, A. Sivasankar Reddy, and S. Uthanna, *Adv. Mater. Lett.* **6**, 834 (2015).
9. JCPDS—International Centre for Diffraction Data, Powder Diffraction File No. 05-0667 (1996).
10. V. Balkanski, V. A. Nusimovici, and J. Reydelle, *Solid State Commun.* **7**, 815 (1969).
11. A. Compaan and H. Z. Commins, *Phys. Rev. B* **6**, 4753 (1972).
12. P. Y. Yu, Y. R. Shen, and Y. Petroff, *Solid State Commun.* **12**, 973 (1973).
13. S. P. S. Porto and P. F. Williams, *Phys. Rev. B* **8**, 1782 (1973).
14. P. Y. Yu and Y. R. Shen, *Phys. Rev. Lett.* **32**, 376 (1974).

Translated by E. Smorgonskaya